Electronic Supplementary Material (ESI) for Journal of Materials Chemistry A.

Conductive Metal–Organic Framework Nanowires Array for Electrocatalytic Oxygen Evolution

Wen-Hua Li, Jiangquan Lv, Qiaohong Li, Jiafang Xie, Naoki Ogiwara , Yiyin Huang, Huijie Jiang, Hiroshi Kitagawa, Gang Xu* and Yaobing Wang*

Table of Contents

1. Supplementary Figures:

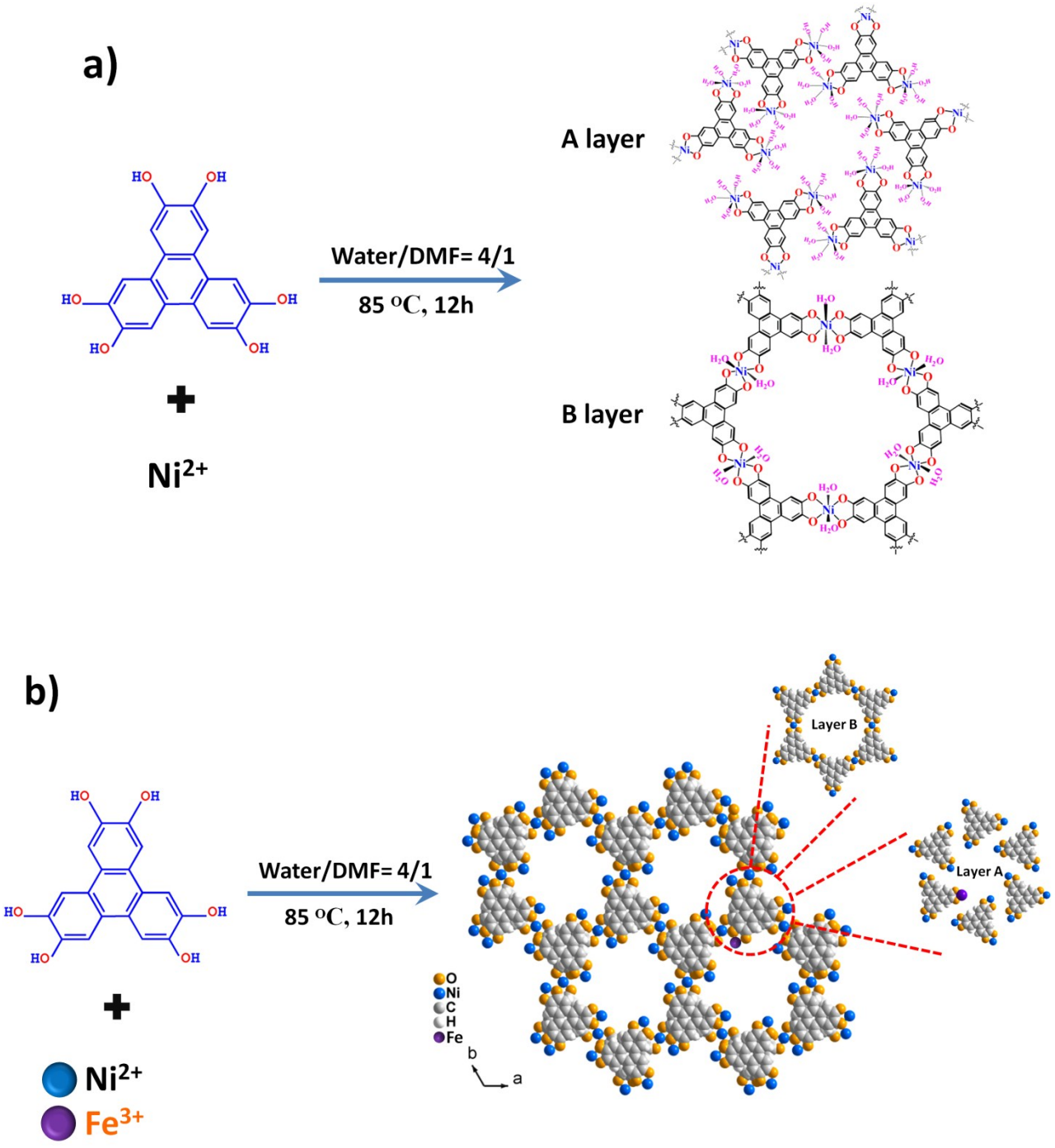

Figure S1. a)The scheme of hydrothermal method to synthesis Ni-HHTP. A layer is discrete layer and B layer is continuous layer. b) Scheme for the synthesis of FexNiy-HHTP.

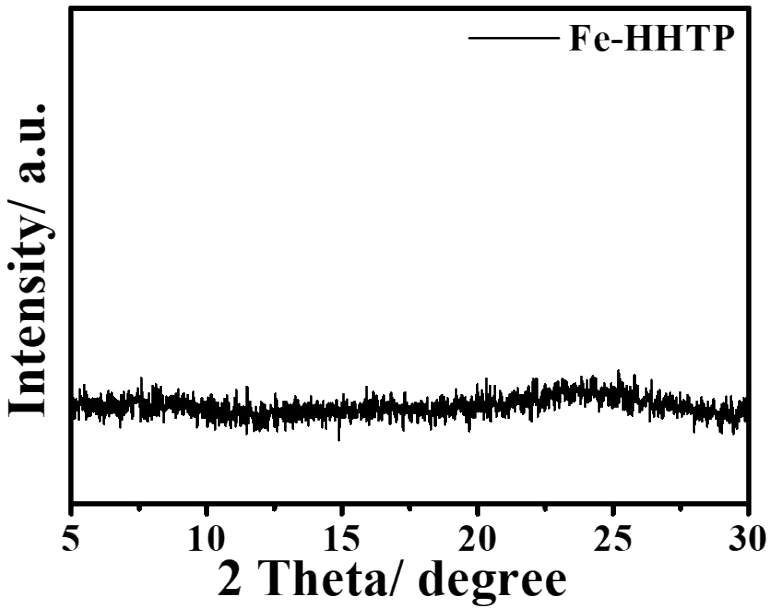

Figure S2. The PXRD pattern for Fe-HHTP powder shows an amorphous phase, which indicates that Fe-HHTP MOF structure cannot be achieved under the condition applied in the manuscript.

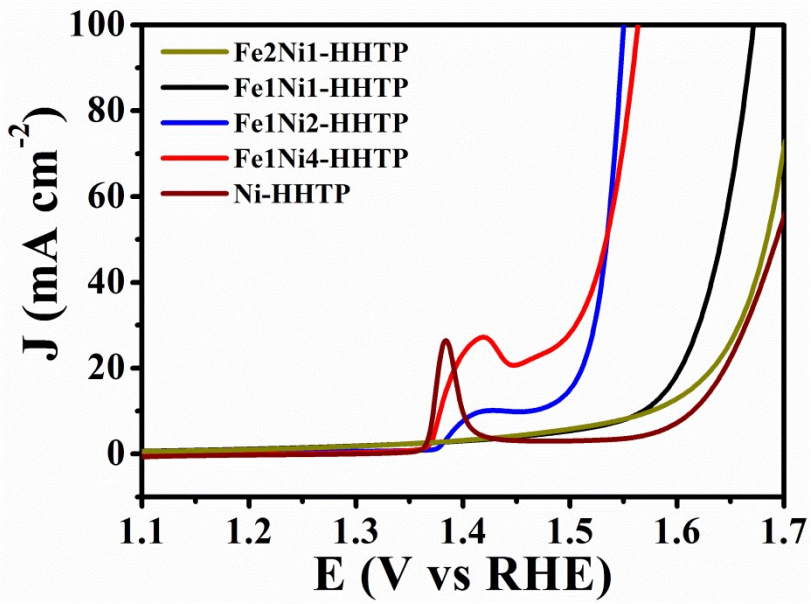

Figure S3. LSV curves of Ni-HHTP, Fe1Ni4-HHTP, Fe1Ni2-HHTP, Fe1Ni1-HHTP, Fe2Ni1-HHTP in 1 M KOH.

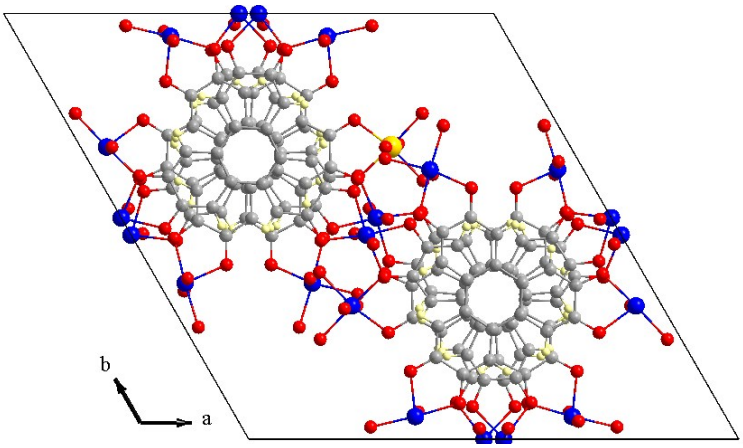

Figure S4. A possible unit cell of Fe1Ni4-HHTP, which is almost the same as Ni-HHTP except one Ni was substitute by one Fe in the discrete layer. A and B layer stacked in sequence and are crystallized in the trigonal space group of $P\bar{3}c1$ (Blue atom for Ni, yellow atom for Fe, grey atom for carbon, light yellow atom for hydrogen).

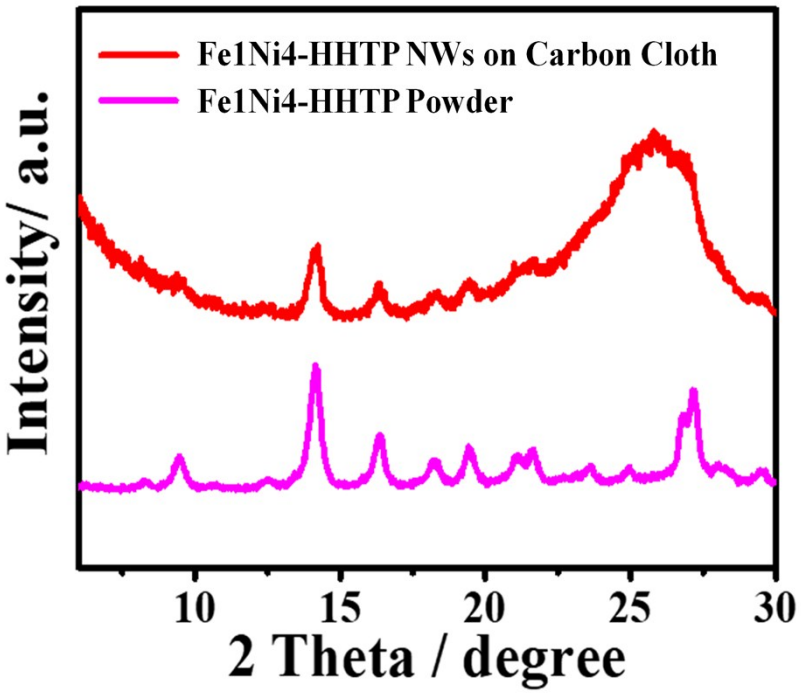

Figure S5. PXRD patterns for Fe1Ni4-HHTP powder and Fe1Ni4-HHTP NWs on carbon cloth. The matching peaks of two patterns demonstrate the successful synthesis of FeNi-HHTP on carbon cloth. (The broad peak in red line belongs to the carbon clothes substrate)

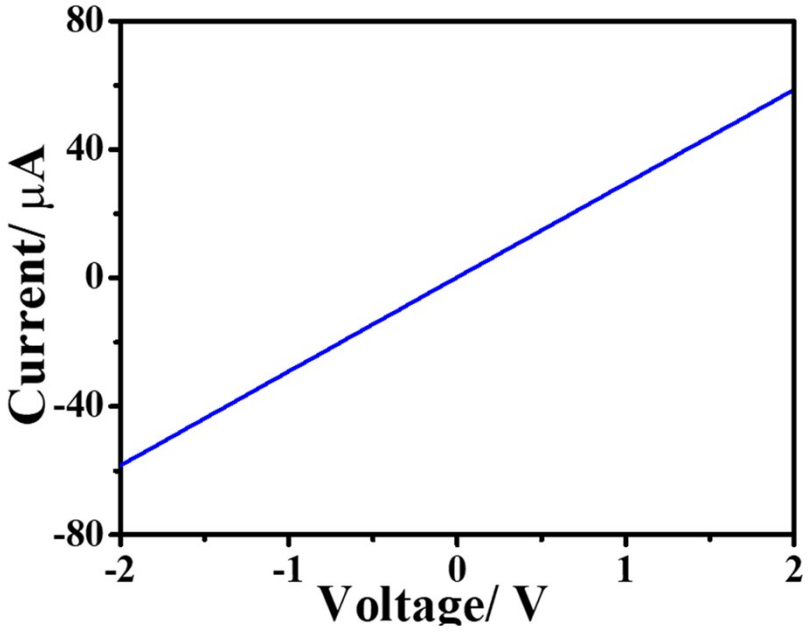

Figure S6. Electrical measurements of Ni-HHTP were performed using two-electrode in air at a constant temperature of 297 K and in the absence of light.The electrical conductivity is calculated to be 3.03×10^{-5} S cm^{-1}.($\sigma = L/(R\times\pi(d/2)^2)$, L = 0.50 mm, d = 2.5 mm, R = 3.3×10^4 Ω) .

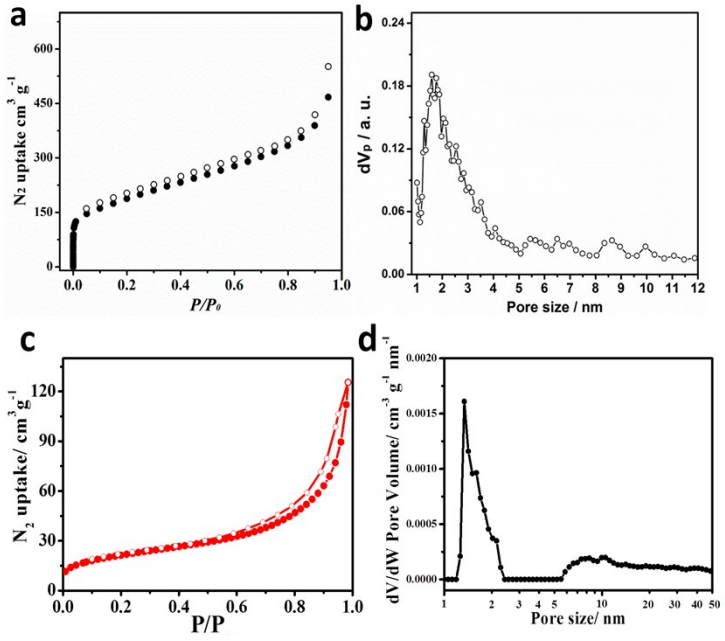

Figure S7. (a, b) N_2 sorption isotherms and pore size distribution(from NLDFT fitting) of Ni-HHTP at 77 K .(c, d) N_2 sorption isotherms and pore size distribution(from NLDFT fitting) of Fe1Ni4-HHTP at 77 K .

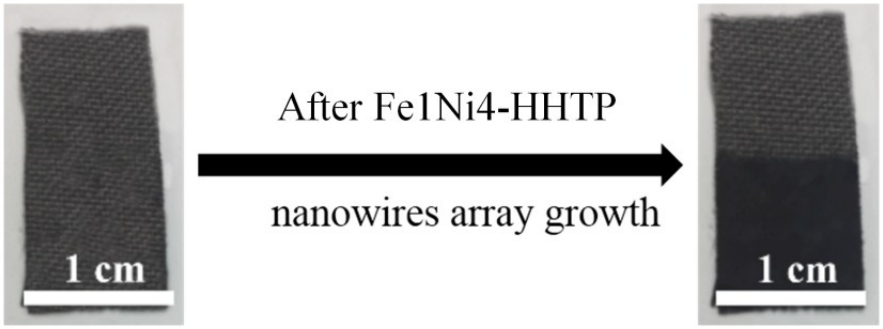

Figure S8. The obvious change on carbon cloth from grey to dark blue after the growth of Fe1Ni4-HHTP nanowires array with controlled 1×1 cm^2.

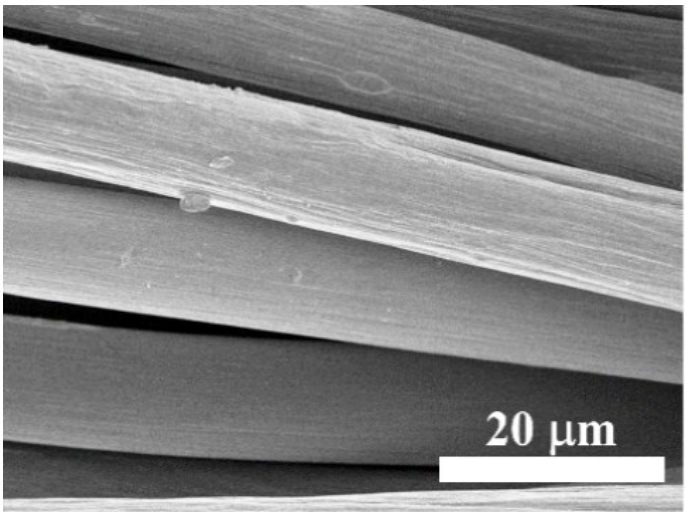

Figure S9. SEM image of bare carbon cloth shows smooth surfaces.

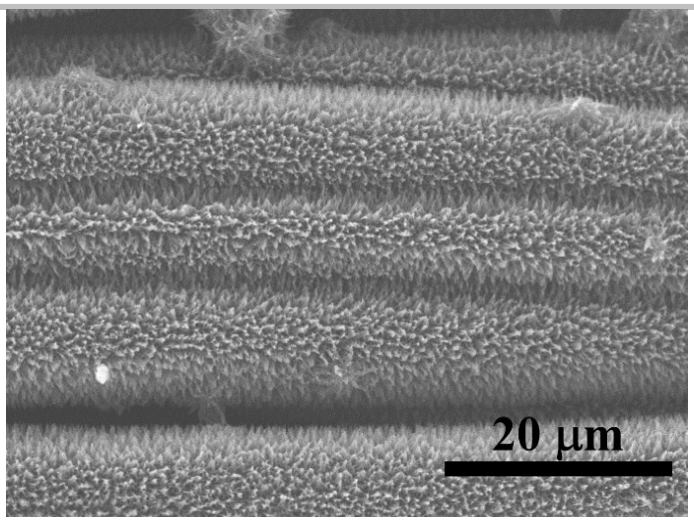

Figure S10. SEM images of the Fe1Ni4-HHTP nanowires array growing on carbon cloth.

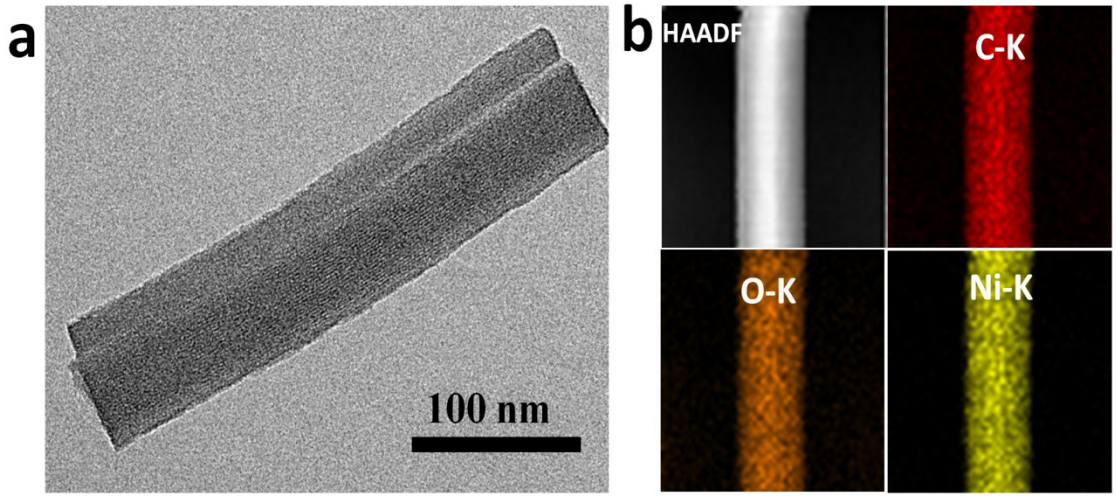

Figure S11. (a) HRTEM of Ni-HHTP nanowire; (b) HAADF-STEM image and corresponding C-K, O-K, Ni-K, STEM-EDX map in Ni-HHTP nanowires .

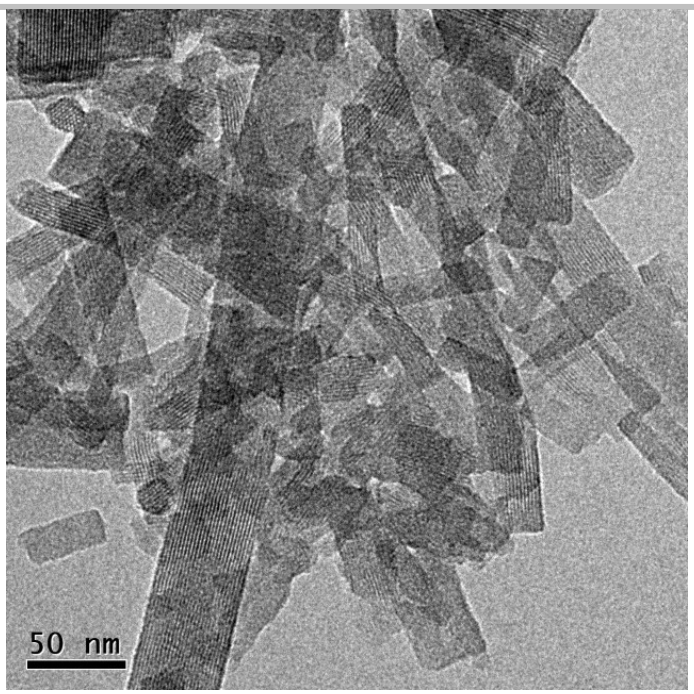

Figure S12. HRTEM image of Fe1Ni4-HHTP nanowires array

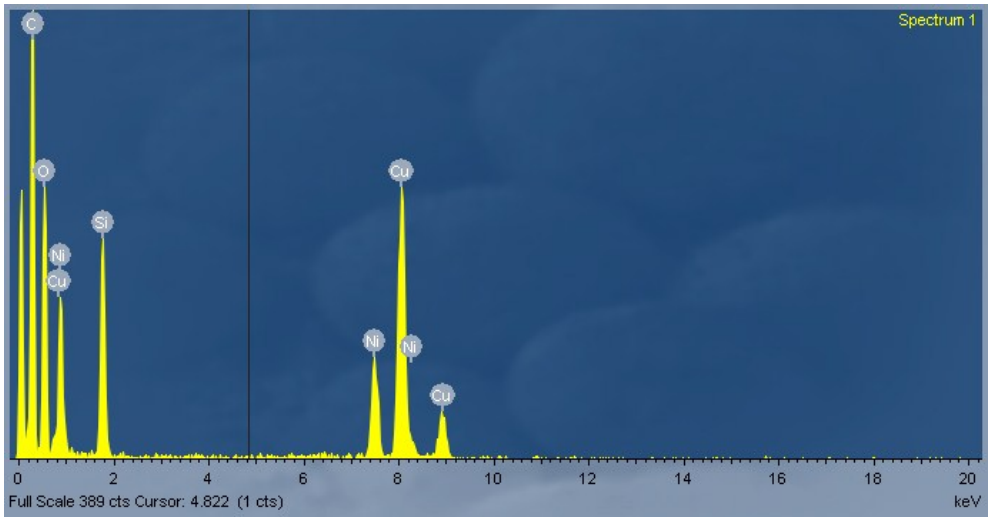

Figure S13. EDS spectrum of Ni-HHTP nanowires array.

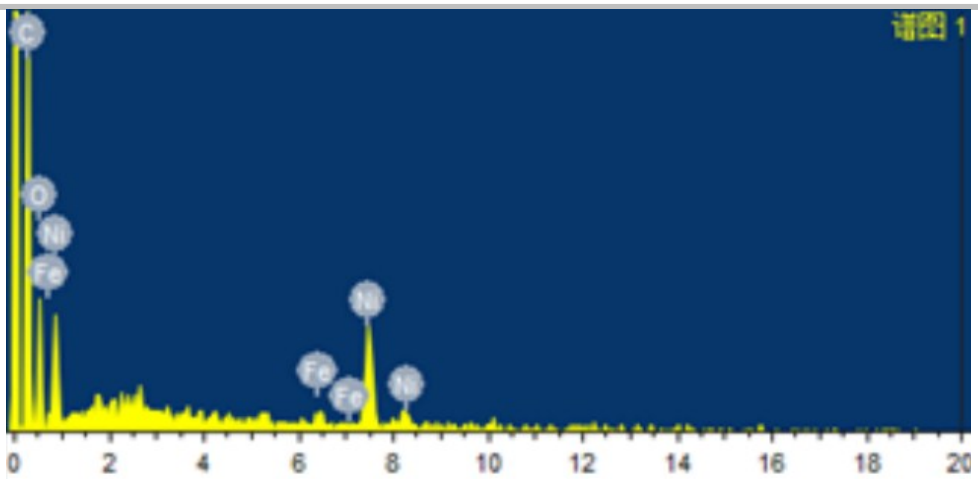

Figure S14. EDS spectrum of Fe1Ni4-HHTP nanowires array.

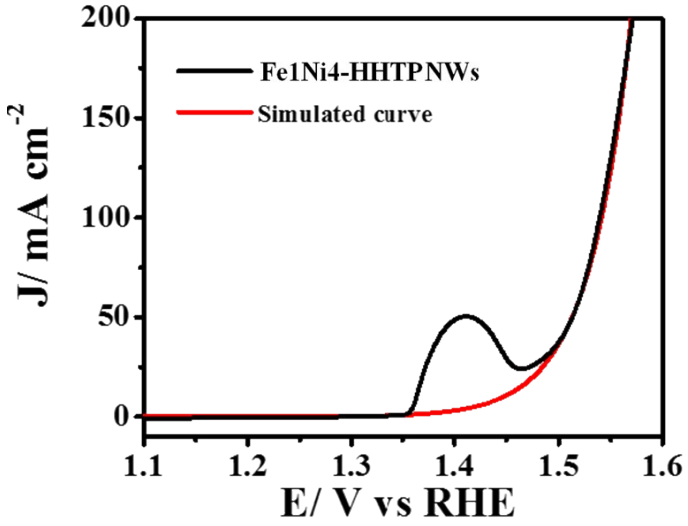

Figure S15. LSV curve of Fe1Ni4-HHTP NWs (black line) and the corresponding simulated curve (red line) to obtain overpotential of 213 mV at 10 mA cm^{-2}.

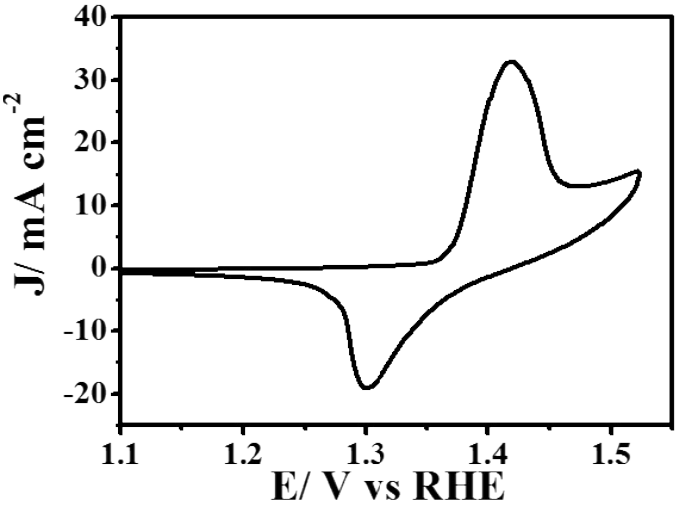

Figure S16. CV of Fe1Ni4-HHTP NWs, which showed a characteristic $Ni^{2+/3+}$ redox couple

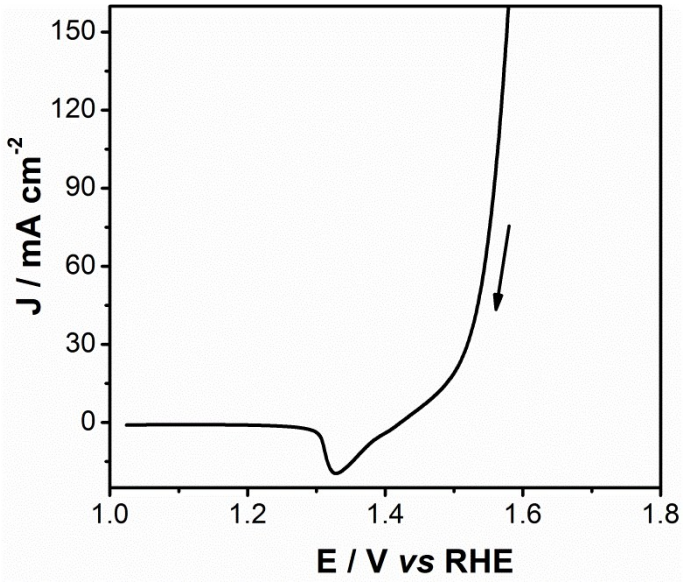

Figure S17 The LSV curve of Fe1Ni4-HHTP NWs at a reversed scan direction in 1M KOH.(Scan rate: 10 mV s-1)

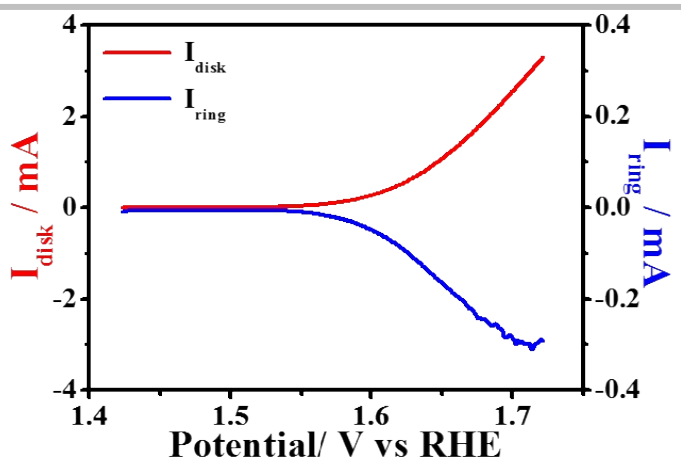

Figure S18. Faraday efficiency testing of Fe1Ni4-HHTP NWs using the RRDE technique in N_2-saturated 1 M KOH solution. Faradaic efficiency measurements were calculated at I_d = 0.2 mA, and the corresponding FE=98.1%.

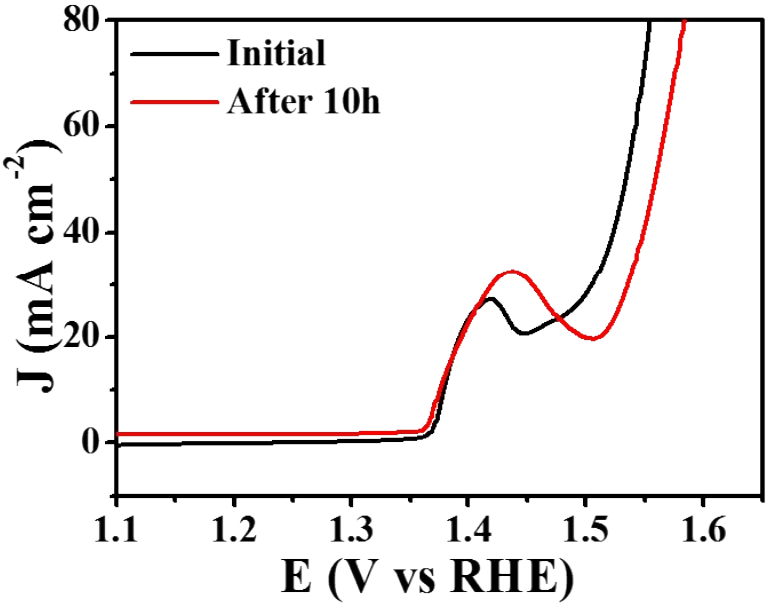

Figure S19. LSV curves of Fe1Ni4-HHTP NWs *in situ* grown on carbon cloth before and after 10 h durability test at 30 mA cm^{-2}.

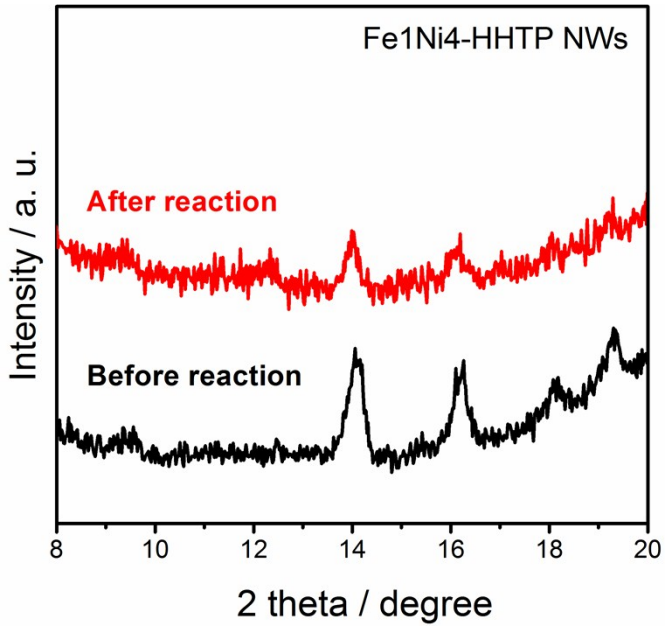

Figure S20. PXRD patterns of Fe1Ni4-HHTP NWs before and after OER process.

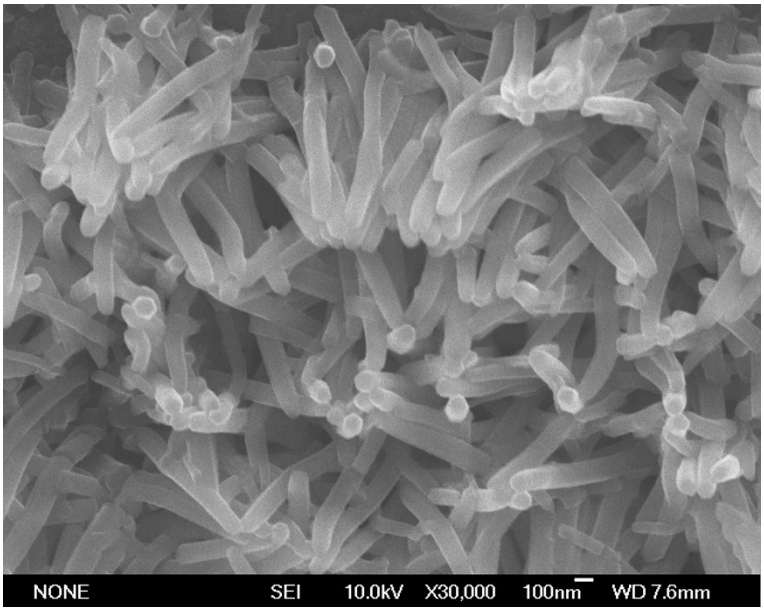

Figure S21. SEM image of Fe1Ni4-HHTP NWs after OER process.

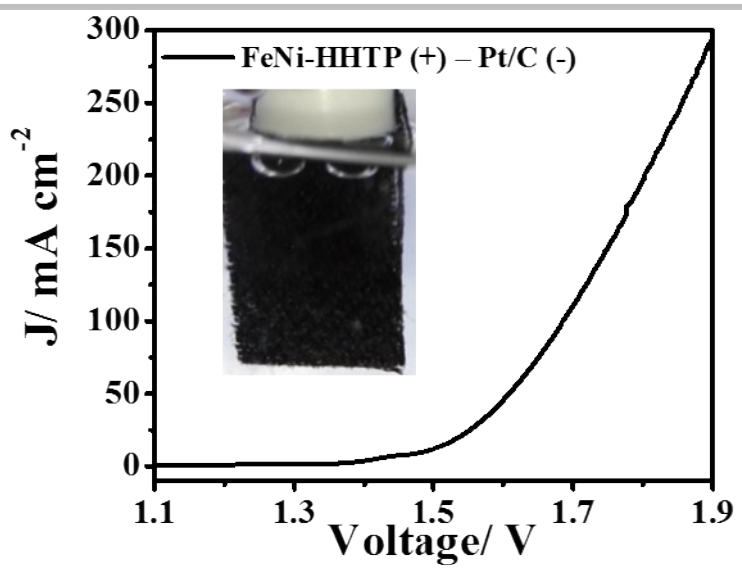

Figure S22. Steady-state polarization curves for overall water splitting of Fe1Ni4-HHTP NWs and Pt/C in a two-electrode configuration (Inset: the photograph shows the evolution of oxygen gas bubbles).

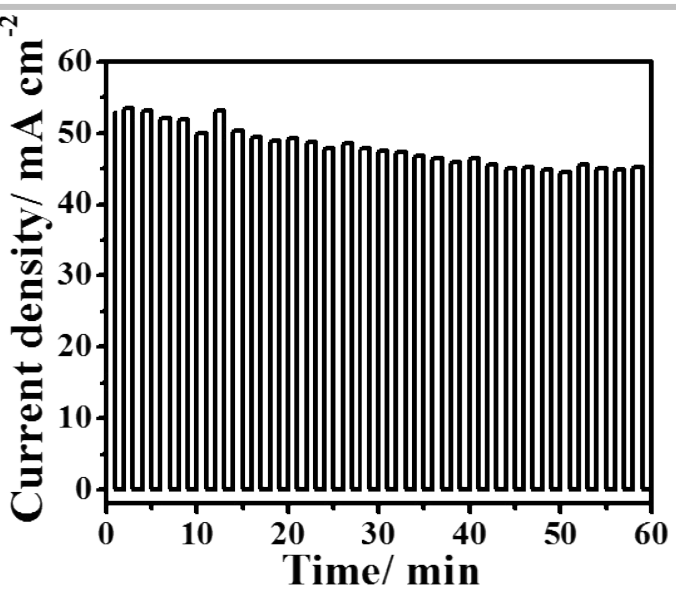

Figure S23. The measured current density during the solar cell driven overall water splitting under chopped simulated sunlight (AM 1.5G), the data were recorded for the time period of 1h.The solar-to-hydrogen conversion efficiency (η_{SHE}) was determined by coupling the electricity-to-hydrogen efficiency (η_{elec}) with solar cell efficiency (η_{solar}), reaching up to 9.2% using Fe1Ni4-HHTP NWs as anode

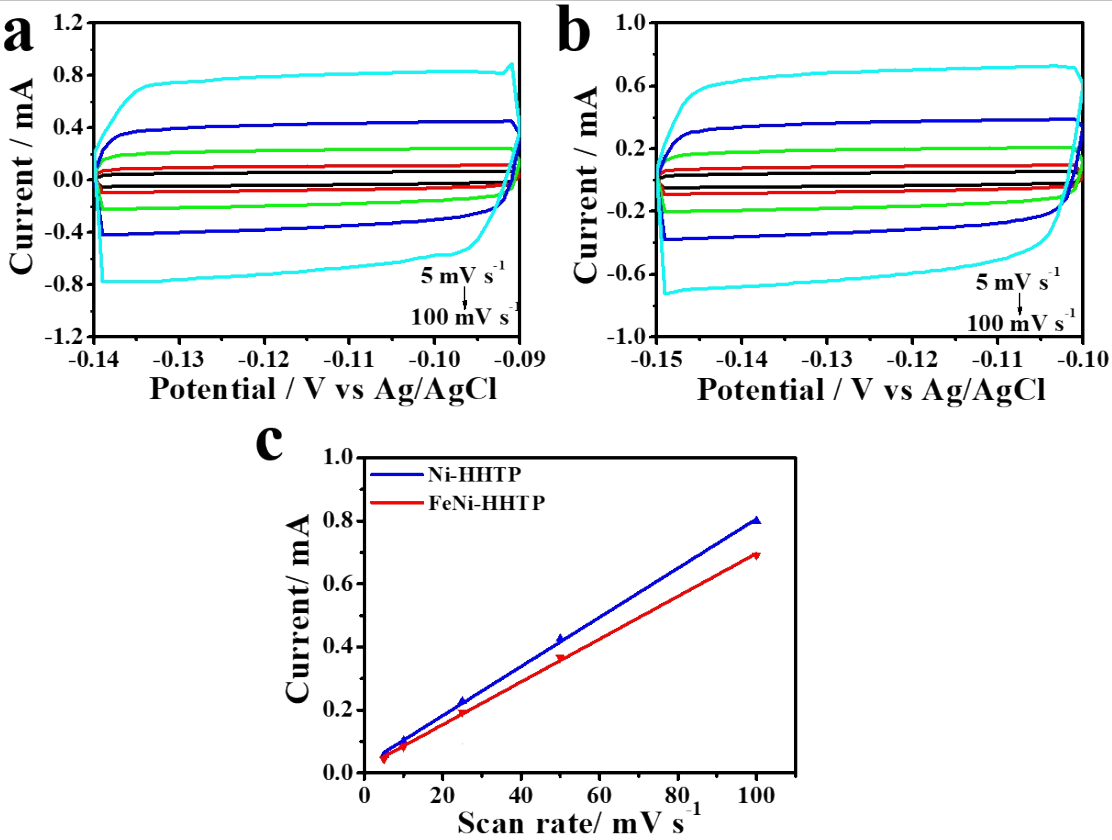

Figure S24. CV curves of (a) Ni-HHTP NWs and (b) Fe1Ni4-HHTP NWs were measured in a non-Faradaic region at the following scan rates: 5, 10, 25, 50 and 100 mV s^{-1}; (c) the corresponding figure for the differences in current density variation plotted against scan rate fitted to a linear regression enables the estimation of C_d.

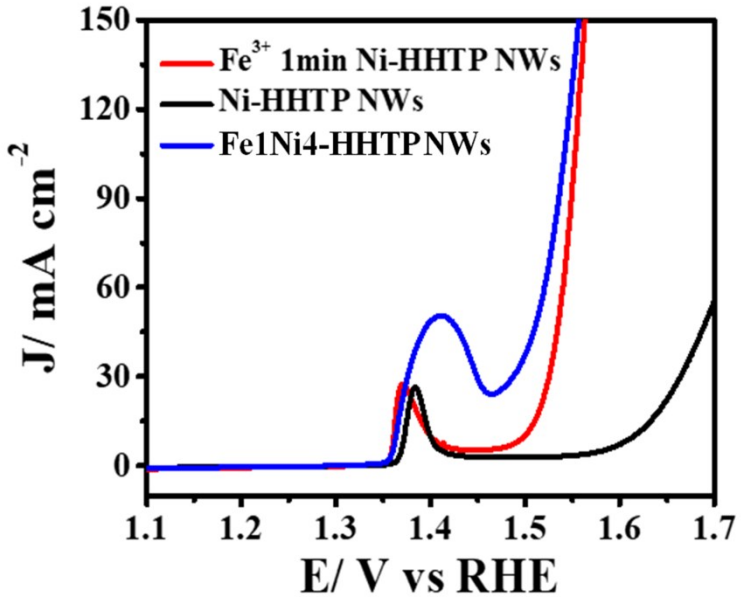

Figure S25. LSV curves of Ni-HHTP NWs, Fe1Ni4-HHTP NWs and Ni-HHTP dipping in Fe^{3+} solution for 1 min (wash sevel times before test).

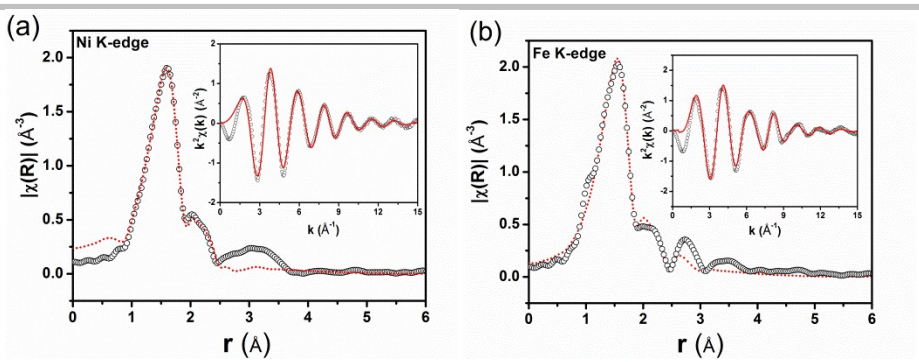

Figure S26. RDF of Fe1Ni4-HHTP (black circle) and fitting (red line).

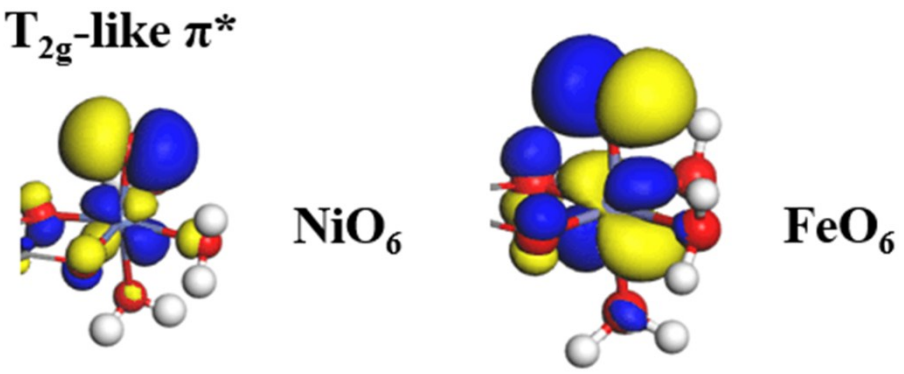

FigureS27. Computed LUMO for Fe1Ni4-HHTP and Ni-HHTP electrocatalysts respectively.

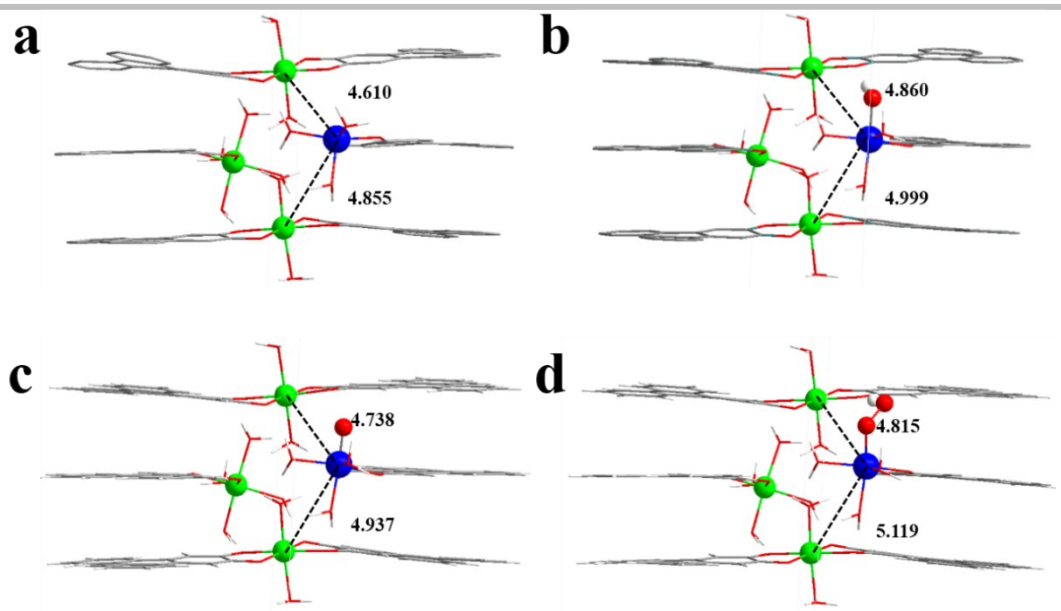

Figure S28. The relative distance of Fe active site and two neighbor layer Ni during different OER processes of (a) Fe* vacancy; (b) OH* absorption; (c)O* formation; (d) OOH* formation.

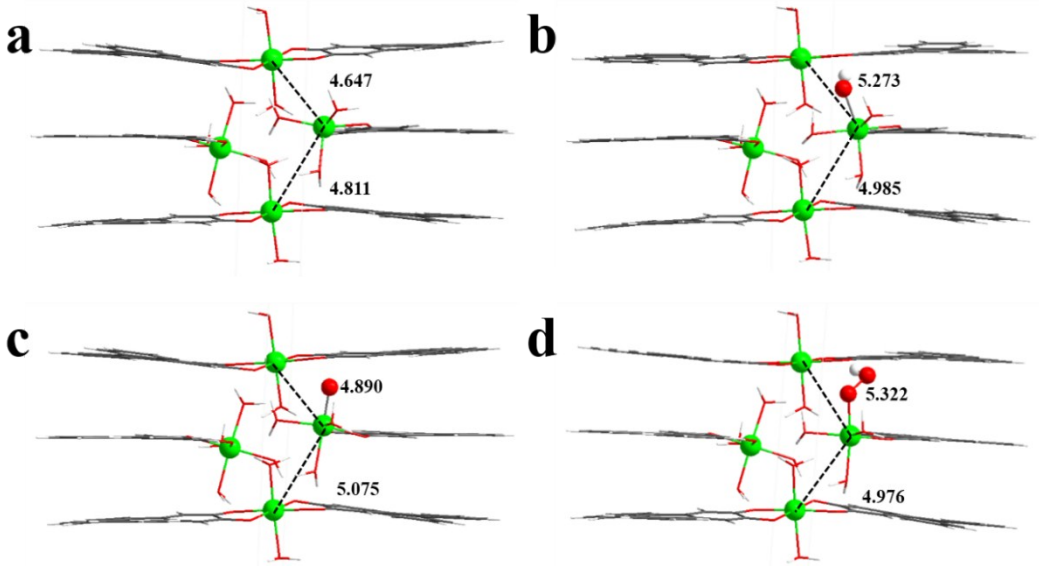

Figure S29. The relative distance of Ni active site and two neighbor layer Ni during different OER processes of (a) Fe* vacancy formation; (b) OH* absorption; (c) O* formation; (d) OOH* formation.

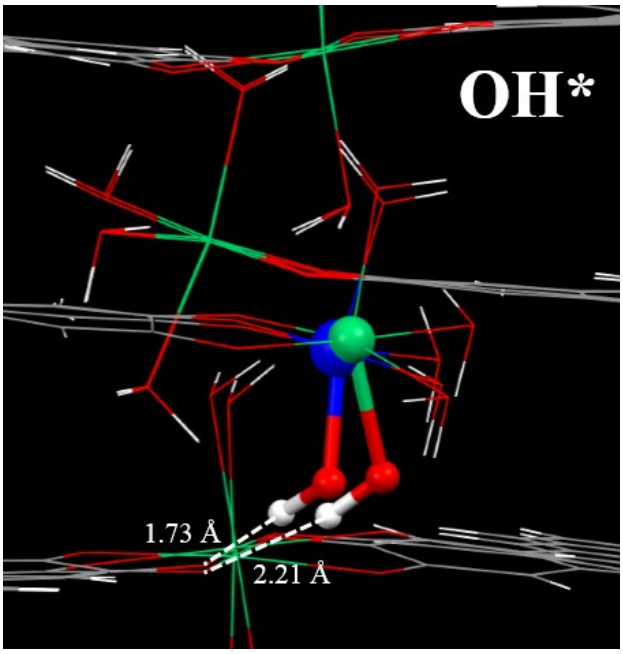

Figure S30. The overlap of Fe1Ni4-HHTP (Fe: blue atom) and Ni-HHTP (Ni: green atom) structures to show the different hydrogen bond distances between OH* intermediate and neighbor O atom.

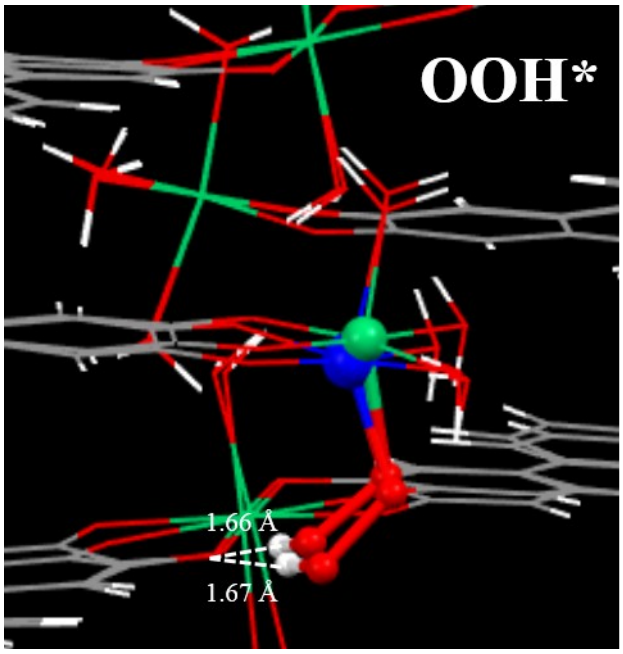

Figure S31. The overlap of Fe1Ni4-HHTP (Fe: blue atom) and Ni-HHTP (Ni: green atom) structures to show the different hydrogen bond distances between OOH* intermediate and neighbor O atom.

2. Supplementary Tables

Table S1. ICP-OES results of Fe1Ni4-HHTP nanowires array

Sample Information	Fe1Ni4-HHTP
Elements	Fe, Ni
Equipments	ICP- OES spectrometer, Ultima 2
Limit of detection	0.5ppb
Results	Fe/Ni = 0.665/10.05

The inductively coupled plasma optical emission spectroscopy (ICP-OES) analysis reveal that 6.9% Ni was replaced by Fe in Fe1Ni4-HHTP nanowires.

Table S2. Comparison of the OER activity for the synthesized Fe1Ni4-HHTP nanowires array with several recently reported MOF OER electrocatalysts.

Catalyst	Overpotentials (V)	Current density (mA cm^{-2})	Solution	Substrate	Reference
Fe1Ni4-HHTP NWs	0.210	10	1 M KOH	Carbon cloth	**This work**
NiCo-UMOFNs	0.189	10	1 M KOH	Cu foam	S1
MAF-X27-OH (Cu)-3	0. 292	10	1 M KOH	Cu foil	S2
Fe_3-Co_2@GC	0.283	10	0.1 M KOH	GC	S3
2D Co-MOF	0. 293	10	0.1 M KOH	GC	S4
NNU-23	0.365	10	0.1 M KOH	GC	S5
$A_{2.7}$B-MOF-$FeCo_{1.6}$	0.288	10	1 M KOH	Ni foam	S6

Table S3. Fitting parametres of Ni K-edge and Fe K-edge EXAFS curve for Ni-HHTP, Fe1Ni4-HHTP, Fe-HHTP, and their references are showed in the table S3..

Sample	Path	C.N.	R (Å)	$\sigma^2 \times 10^3$ (Å^2)	ΔE (eV)	R factor
Ni foil	Ni-Ni	12*	2.48±0.001	6.2±0.1	0.8±0.1	0.0003
NiO	Ni-O	7.9±1.0	2.09±0.01	6.7±1.7	-0.6±1.6	0.006
	Ni-Ni	16.7±1.3	2.95±0.01	6.9±0.6	-3.4±0.8	
Ni-HHTP	Ni-O	7.4±0.5	2.05±0.01	6.8±0.9	-4.2±0.8	0.010
	Ni-C	3.3±0.9	2.80±0.03			
Fe1Ni4-HHTP	Ni-O	7.3±0.5	2.05±0.01	6.9±0.9	-4.4±0.8	0.008
	Ni-C	2.8±0.9	2.81±0.03			
Fe foil	Fe-Fe	8*	2.47±0.01	5.1±0.7	6.4±1.3	0.005
		6*	2.84±0.01	6.3±1.3	5.7±2.4	
FeO-1	Fe-O	4.5±0.3	2.12±0.01	12.9±0.9	1.8±0.6	0.008
	Fe-Fe	10.1±0.9	3.07±0.01			
α-Fe2O3	Fe-O	8.1±1.6	1.95±0.02	13.2±2.6	-12.0±2.5	0.011
γ-Fe2O3	Fe-O	6.0±0.7	1.93±0.01	11.0±1.6	-5.8±1.6	0.003
Fe3O4	Fe-O	4.7±0.5	2.01±0.02	10.7±1.1	-0.67±2.0	0.012
	Fe-Fe	4.2±0.7	2.97±0.02			
	Fe-Fe	12.6±1.4	3.47±0.01			
Fe-HHTP	Fe-O	8.4±0.6	2.00±0.01	9.4±1.0	-2.6±0.7	0.005
	Fe-C	2.3±0.8	2.84±0.04			
Fe1Ni4-HHTP	Fe-O	7.9±0.8	2.01±0.01	6.9±1.2	0.9±1.1	0.014
	Fe-C	5.5±2.0	2.78±0.03			
	Fe-C/O	12.4±7.7	3.03±0.02			

* The data for Fe foil and Ni foil was first fitted with the coordination number fixed to determine the amplitude reduction factor (S_0^2=0.77 for Fe and S_0^2=0.83 for Ni) for the fitting of other samples. The k range was set between 3 – 15 Å^{-1}, R range of 1-3 Å. Independent CN and bond lenght were used for every shell, and the Debye-Waller factor and energy shift were shared for a dataset. A k weighting of 2 was used for all the fitting, and no parameters (CN, R, σ^2, ΔE_0) was fixed.

Table S4. The distance between active site (Fe/Ni) and two neighbor layer Ni during four primitive steps of the OER process

	Ni-HHTP		Fe1Ni4-HHTP	
	A layer (Å)	B layer (Å)	A layer (Å)	B layer (Å)
$M_{vacancy}$*	4.647	4.855	4.610	4.855
OH*	5.273	4.985	4.860	4.999
O*	4.890	5.075	4.738	4.937
OOH*	5.322	4.976	4.815	5.119

3. References

[S1] S. L. Zhao, Y. Wang, J. C. Dong, C. T. He, H. J. Yin, P. F. An, K. Zhao, X. F. Zhang, C. Gao, L. J. Zhang, J. W. Lv, J. X. Wang, J. Q. Zhang, A. M. Khattak, N. A. Khan, Z. X. Wei, J. Zhang, S. Q. Liu, H. J. Zhao, Z. Y. Tang, Nat Energy 2016, 1, 1-10

[S2] Xue-Feng Lu, Pei-Qin Liao, Jia-Wei Wang, Jun-Xi Wu, Xun-Wei Chen, Chun-Ting He, Jie-Peng Zhang*, Gao-Ren Li*, and Xiao-Ming Chen, An Alkaline-Stable, Metal Hydroxide Mimicking Metal–Organic Framework for Efficient Electrocatalytic Oxygen Evolution. J. Am. Chem. Soc., 2016, 138 (27), pp 8336–8339

[S3] Jian-Qiang Shen, Pei-Qin Liao*, Dong-Dong Zhou, Chun-Ting He, Jun-Xi Wu, Wei-Xiong Zhang, Jie-Peng Zhang* , and Xiao-Ming Chen Modular and stepwise synthesis of a hybrid metal–organic framework for efficient electrocatalytic oxygen evolution. J. Am. Chem. Soc., 2017, 139 (5), pp 1778–1781

[S4] Zhu AX, Dou AN, Fang XD, Yang LB, Xu QQ. Chemical etching of a cobalt-based metal-organic framework for enhancing the electrocatalytic oxygen evolution reaction (vol 5, pg 24016, 2017) (Retraction of Vol 5, Pg 24016, 2017). J Mater Chem A 2017, 5(45): 24016-24016.

[S5] Wang XL, Dong LZ, Qiao M, Tang YJ, Liu J, Li YF, et al. Exploring the Performance Improvement of the Oxygen Evolution Reaction in a Stable Bimetal-Organic Framework System. Angew Chem Int Edit 2018, 57(31): 9660-9664.

[S6] Xue Z, Li Y, Zhang Y, Geng W, Jia B, Tang J, et al. Modulating Electronic Structure of Metal-Organic Framework for Efficient Electrocatalytic Oxygen Evolution. Adv Energy Mater 2018, 8(29): 1801564.

Author Contributions

The contributions of authors to this work are as follows: Wen-Hua Li designed and performed synthesis experiments, characterization and data analysis. Jiangquan Lv performed the electrochemical properties measurements. Wen-Hua Li, Jiangquan Lv, Gang Xu and Yaobing Wang wrote the manuscript. Qiaohong Li helped with the DFT calculation. Jiafang Xie helped to analyze the electrochemical data. Yiyin Huang and Huijie Jiang performed partial synthesis work. Hiroshi Kitagawa and Naoki Ogiwara performed XAS measurements. Gang Xu and Yaobing Wang are in charge of the manuscript.